

# Articles

## Structural and Electronic Properties of Co-corrole, Co-corrin, and Co-porphyrin

Carme Rovira,<sup>†,‡</sup> Karel Kunc,<sup>‡,§</sup> Jürg Hutter,<sup>‡,||</sup> and Michele Parrinello<sup>\*,‡</sup>

Departament de Química Física, Universitat de Barcelona, Martí i Franquès 1, 08028 Barcelona, Spain, Max-Planck-Institut für Festkörperforschung, Heisenbergstrasse 1, 70569 Stuttgart, Germany, Laboratoire d'Optique des Solides (CNRS), Université Pierre et Marie Curie, 4 Place Jussieu, 75252 Paris Cedex 05, France, and Institute of Organic Chemistry, University of Zurich, Winterthurerstrasse 190, 8057 Zurich, Switzerland

Received February 9, 2000

A quantitative study of the structure and electronic properties of Co-corrole, Co-corrin, and Co-porphyrin, using density functional theory, is reported. The structure of each macrocycle is optimized, with no symmetry constraints, by considering different spin states. The ground-state structures and spin states ( $S = 1$  for Co-corrole,  $S = 0$  for Co-corrin and  $S = 1/2$  for Co-porphyrin) are in good agreement with the experimental data available. The trends in the sizes of the coordination cavities upon varying the inner metal atom and/or the macrocycle are analyzed and compared with those for the Fe-porphyrin we studied previously. Our results reveal that most of the distortion of the Co-corrin core in the B<sub>12</sub> coenzyme is due to the inherent properties of Co-corrin. Quite different behaviors are found between corrinoids and porphyrins upon varying the spin state. While an increase in the metal–nitrogen (M–N) distance with spin state occurs in the porphyrins, the corrinoids show little variation in the M–N distance and, in some cases, undergo small structural changes in the ring structure. These results aid in understanding the often discussed question of why nature has chosen corrin/porphyrin for carrying out the particular biological functions identified in the B<sub>12</sub> coenzyme.

### Introduction

Corrinoids are macrocyclic molecules built from a tetrapyrrolic ring with two directly connected pyrroles.<sup>1</sup> They are of interest as optoelectronic devices and have been used in catalytic applications,<sup>2,3</sup> and one of them (Co-corrin) has been chosen by nature to carry out essential biological functions, viz., those catalyzed by the B<sub>12</sub>-dependent enzymes.<sup>4,5</sup> The coenzyme B<sub>12</sub> molecule contains a corrin macrocycle, the most saturated among all the corrinoids, which is coordinated to a cobalt atom (Figure 1b). The search for functional analogues of the B<sub>12</sub> coenzyme has led to an important area of research based on the synthesis of similar corrinoid ligands.<sup>1</sup> An interesting member of this family is corrole (Figure 1a), which is the most unsaturated one.

An intriguing question is why nature uses corrin for carrying out specific functions rather than one of many other macrocycles, such as porphyrin (Figure 1c), that are widely used in biological processes. As possible explanations, the flexibility of the corrin macrocycle, its smaller “cavity size”, and steric

interactions induced by the macrocycle have been often proposed.<sup>1,6</sup> In this context, it has been suggested that it is because of the loss of aromaticity that the corrin ring is more flexible than both the corrole and the porphyrin rings.<sup>6c,d</sup> Indeed, the flexibility of the macrocycle may facilitate the homolytic cleavage of the Co–C bond in the coenzyme, which is the first step of all rearrangement reactions catalyzed by the B<sub>12</sub>-dependent enzymes. Another proposition is that only corrin can supply a cavity size capable of accommodating the cobalt atom. Furthermore, it has been suggested that the steric interactions exerted by the corrin ring trigger the above processes.<sup>7</sup> This is supported by the fact that the X-ray structure of the B<sub>12</sub> coenzyme reveals a particularly constrained interaction between the 5'-deoxyadenosyl group and the atoms of the corrin ring,<sup>8</sup> although a more recent spectroscopic study challenges this hypothesis.<sup>5</sup>

As a first step toward resolving these issues, acquiring a quantitative knowledge of the intrinsic structural and electronic properties of the Co-corrin macrocycle, in the context of other

<sup>†</sup> Universitat de Barcelona.

<sup>‡</sup> Max-Planck-Institut für Festkörperforschung.

<sup>§</sup> Université Pierre et Marie Curie.

<sup>||</sup> University of Zurich.

(1) Liccoccia, S.; Paolesse, R. *Struct. Bonding* **1995**, *84*, 71.

(2) Sessler, J. *Angew. Chem., Int. Ed. Engl.* **1994**, *106*, 1410.

(3) Murayami, Y.; Aoyama, Y.; Hayashida, M. *J. Chem. Soc., Chem. Commun.* **1980**, 501.

(4) Stryer, L. *Biochemistry*, 4th ed.; Freeman: New York, 1995.

(5) Dong, S.; Padmakumar, R.; Banerjee, R.; Spiro, T. G. *J. Am. Chem. Soc.* **1999**, *121*, 7063–7070.

(6) (a) Geno, M. K.; Halpern, J. *J. Am. Chem. Soc.* **1987**, *109*, 1238–1240. (b) Halpern, J. *Science* **1985**, *227*, 869. (c) Stolzenberg, A. M.; Stershic, M. T. *J. Am. Chem. Soc.* **1988**, *110*, 6391. (d) Murakami, Y.; Aoyama, Y.; Tokumaga, K. *J. Am. Chem. Soc.* **1980**, *102*, 6736.

(7) (a) Bresciani-Pahor, N.; Forcolin, M.; Marzilli, L. G.; Randaccio, L.; Summers, M.; Toscano, P. *J. Coord. Chem. Rev.* **1985**, *63*, 1–125. (b) Polson, S. M.; Hansen, L.; Marzilli, L. *J. Am. Chem. Soc.* **1996**, *118*, 4804–4808. (c) Tsou, T. T.; Loots, M.; Halpern, J. *J. Am. Chem. Soc.* **1982**, *104*, 623.

(8) Glusker, J. In *B<sub>12</sub>*; Dolphin, D., Ed.; Wiley: New York, 1982; p 23 and references therein.

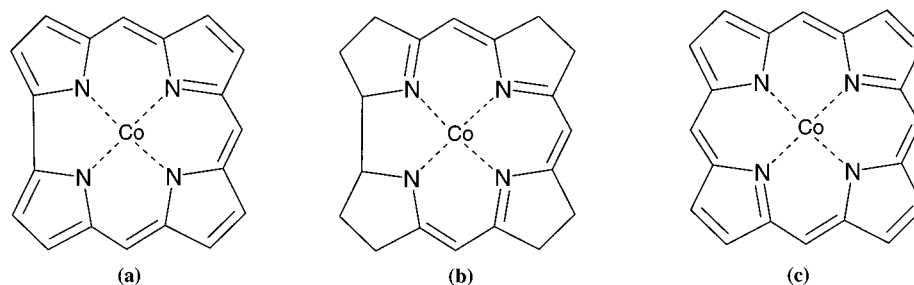


**Figure 1.** Schematic representation of the three cobalt macrocycles studied: (a) Co-corrole; (b) Co-corrin; (c) Co-porphyrin.

closely related macrocycles, would be desirable. Here we report a first-principles study of three cobalt-based macrocycles: Co-corrole, Co-corrin, and Co-porphyrin (Figure 1). They form a series of cobalt complexes with tetrapyrrolic macrocycles which act respectively as tri-, mono-, and dianionic ligands toward the cobalt atom. Our main interest is in comparing the structural and electronic properties of these complexes, as well as their changes with respect to the spin state.

The calculations reported were performed by means of density-functional molecular dynamics within the Car–Parrinello scheme. This is the same computational method that has already been used in the study of heme models.<sup>9</sup> Density functional theory (DFT) has also been applied with success in the study of other metal corrolates such as In-, Ga-, and Sc-corrole.<sup>10</sup> To the best of our knowledge, the cobalt complexes considered here have not, until now, been studied by first-principles methods.

### Computational Details

All calculations presented here are based on density functional theory<sup>11</sup> within the LSD (spin unrestricted) approximation. The Kohn–Sham (KS) orbitals are expanded in a plane-wave (PW) basis set. An initial random distribution of the PW orbital coefficients is taken. The Ceperley–Alder expression for correlation and gradient corrections of the Becke–Perdew type are used,<sup>12</sup> as was done in our previous work on Fe-porphyrin (FeP).<sup>9a</sup> In the case of FeP we found no significant differences in the results with respect to using either the Becke–Perdew or the BLYP functional. It was recently shown<sup>13</sup> that the use of a hybrid functional (B3LYP) decreases the relative energies of the high-spin states of Fe-porphyrin (FeP) derivatives, although the energy ordering of the spin states is maintained. For the systems studied here, the high-spin states lie much higher in energy than those for FeP (>10 kcal/mol) and, thus, a smaller effect is to be expected. We employ *ab initio* pseudopotentials, generated using the Troullier–Martins scheme.<sup>14a</sup> The 3d<sup>7</sup> electrons of Co are treated as valence states and, after some experimentation, only the s and d components of the Co pseudopotential are retained for the calculations. The following core radii, in au, are used: 1.23 for the s, p atomic orbitals of carbon, 1.12 for the s, p atomic orbitals of N, 0.5 for the s atomic orbitals of H, and 1.9, 2.0, 1.6, 1.3674, respectively, for the s, p, d, f atomic orbitals of Co. The

nonlinear core-correction<sup>14b</sup> is used (with core-charge radius of 1.2 au) to improve the transferability of the Co pseudopotential.

We employ the Car–Parrinello molecular dynamics method<sup>15</sup> for optimization of the atomic structures. A successive use of quenching and annealing performed for about 1 ps is necessary to reach a final convergence of  $10^{-5}$  and  $5 \times 10^{-4}$  au for electronic and ionic gradients, respectively. Structure optimizations are performed with no constraints starting from nonsymmetric structures. In all cases, the systems evolve toward the symmetric structures (with  $C_2$  symmetry for Co-corrin,  $C_{2v}$  for Co-corrole, and  $D_{4h}$  for Co-porphyrin). The symmetry is obeyed within  $<0.001$  Å for distances and  $<0.05^\circ$  for angles.

The ground-state electronic configuration for each spin state is extracted from the analysis of the real-space representation of the KS orbitals. This is contrasted with the atomic orbital contributions of each KS orbital obtained by projecting the PW expansions on a minimal basis of atomic states (we project on the pseudoatomic 1s orbital of H, 2s, 2p orbitals of C, N, and O, and 3d, 4s, 4p orbitals of Co).

An extensive study of the convergence of our results with the energy cutoff in the PW expansion is then performed. In a PW calculation this is the equivalent of investigating basis set convergence. To this purpose, the ground and excited states of Co-corrin are successively optimized with different PW cutoffs up to 130 Ry. Figure 2a shows the convergence of the total energy versus PW cutoff for the ground state of Co-corrin and that of the energy differences between the spin states (see inset). The ordering of spin states does not change with the PW cutoff value, and the energy differences change only very slightly. Structural parameters are even less sensitive than energies to the PW cutoff (Figure 2b,c). The cutoff value of 90 Ry is chosen as a compromise between energy and structure convergence and computational cost (energy differences vary by less than 0.1 kcal/mol, and structural parameters show no appreciable change with respect to the results obtained at 130 Ry). Further methodological details can be found in ref 9.

### Results and Discussion

**Co-corrole.** The structure of Co-corrole (Figure 1a) was optimized by assuming different spin states ( $S = 0, 1, 2$ ). Table 1 summarizes the main electronic properties of each spin state. The lowest energy state turned out to be the triplet ( $S = 1$ ), followed by the singlet state at 6.1 kcal/mol and the quintuplet state at 25 kcal/mol.

In all three cases, the structure evolved toward a completely planar structure of  $C_{2v}$  symmetry. Table 2 lists selected structural parameters for each spin state. To the best of our knowledge, there are no structural data available for a four-coordinated Co-corrole. The closest experimental structure is the one of Co(OMTPC)PPh<sub>3</sub>,<sup>16–18</sup> in which the Co atom is five-coordi-

- (9) (a) Rovira, C.; Kunc, K.; Hutter, J.; Ballone, P.; Parrinello, M. *J. Phys. Chem. A* **1997**, *101*, 8914. (b) Rovira, C.; Carloni, P.; Parrinello, M. *J. Phys. Chem. B* **1999**, *103*, 7031. (c) Rovira, C.; Parrinello, M. *Biophys. J.* **2000**, *78*, 93.
- (10) (a) Ghosh, A.; Jynge, K. *Chem.—Eur. J.* **1997**, *3*, 823. (b) For a review of the applications of DFT to porphyrin macrocycles, see: Ghosh, A. *Acc. Chem. Res.* **1998**, *31*, 189.
- (11) (a) Hohenberg, P.; Kohn, W. *Phys. Rev. B* **1964**, *136*, 864. (b) Kohn, W.; Sham, L. J. *Phys. Rev. A* **1965**, *140*, 1133.
- (12) (a) Ceperley, D. M.; Alder, B. J. *Phys. Rev. Lett.* **1980**, *45*, 566. (b) Becke, A. D. *J. Chem. Phys.* **1986**, *84*, 4524. (c) Perdew, J. P. *Phys. Rev. B* **1986**, *33*, 8822.
- (13) (a) Sigfridson, E.; Ryde, U. *J. Biol. Inorg. Chem.* **1999**, *4*, 99. (b) Spiro, T. G.; Kozlowski, P. M. *J. Am. Chem. Soc.* **1998**, *120*, 4524.
- (14) (a) Troullier, N.; Martins, J. L. *Phys. Rev. B* **1991**, *43*, 1993. (b) Louie, S. G.; Froyen, S.; Cohen, M. L. *Phys. Rev. B* **1982**, *26*, 1738.

- (15) (a) Car, R.; Parrinello, M. *Phys. Rev. Lett.* **1985**, *55*, 2471. (b) Galli, G.; Parrinello, M. In *Computer Simulation in Materials Science*; Pontikis, V., Meyer, M., Eds.; Kluwer: Dordrecht, The Netherlands, 1991. See also references therein.
- (16) Paolese, R.; Licocchia, S.; Bandoli, G.; Dolmella, A.; Boschi, T. *Inorg. Chem.* **1994**, *33*, 1171–1176.
- (17) Abbreviations: OMTP = octamethylcorrole; PPh<sub>3</sub> = triphenylphosphine; OEP = orthoethylporphyrin; T<sub>piv</sub>P = pivalamidophenyl; TPP = tetraphenylporphyrin.

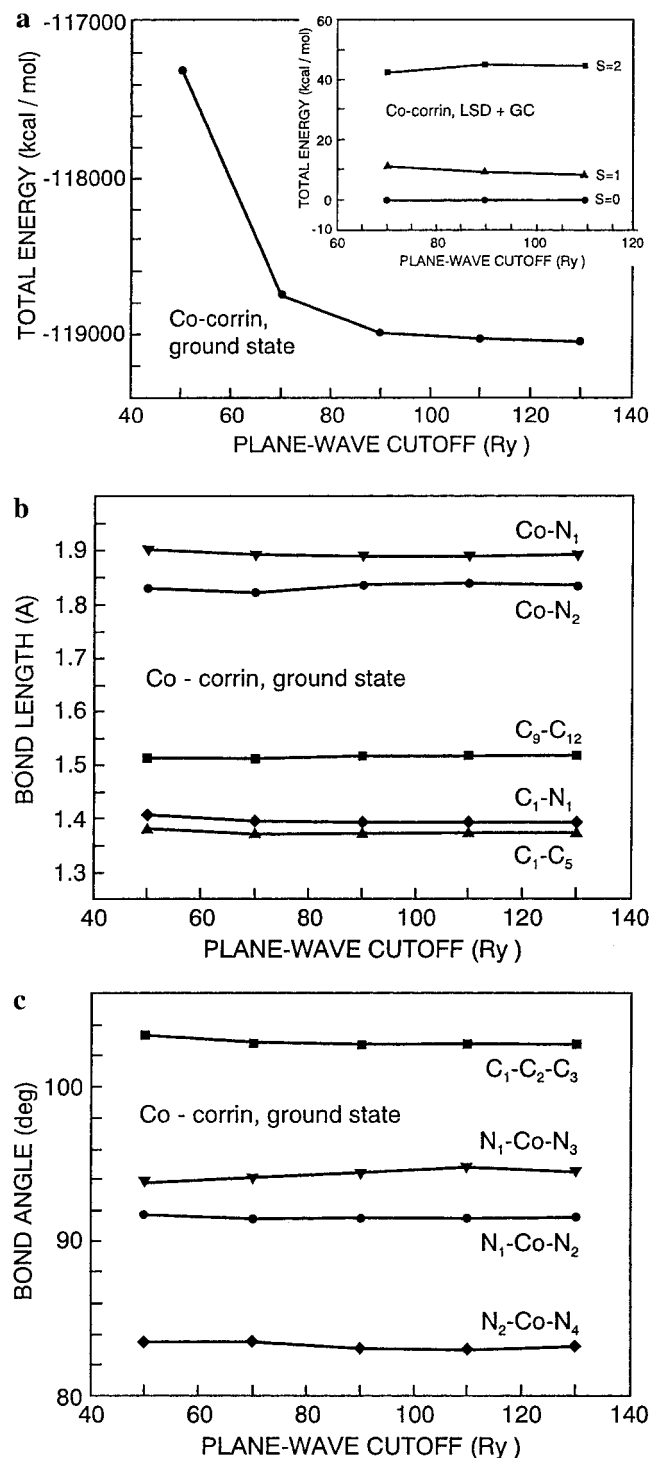


**Figure 2.** (a) Convergence of the total energy and energy differences between different spin states (inset) of Co-corrin with the plane wave (PW) cutoff. (b, c) Variations of selected bonds and angles with the PW cutoff, following the atom-numbering definitions of Table 3).

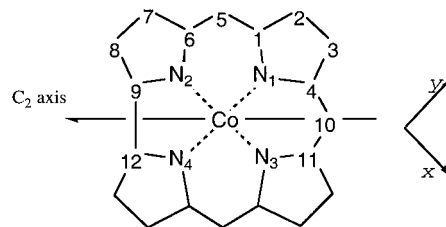
nated. As for other Co-corrinates with bulky substituents, their X-ray structures show a small degree of nonplanarity, which has been attributed to packing steric hindrance.<sup>1</sup> Table 2 shows that the structure of Co(OMTPC)PPh<sub>3</sub> is quite similar to that of the isolated Co-corrin. The largest discrepancies, found for the Co-N distances, most likely reflect the different coordina-

**Table 1.** Metal-Nitrogen (M-N) Distances (Å), Bond Orders, Spin State Energies (kcal/mol), and Formal Oxidation States of the Metal Atoms for Co-corrin, -corrole, and -porphyrin<sup>a</sup>

| macrocycle and spin state | M-N length | M-N bond order | $E_{rel}$ | M formal oxidn state                | $d_{x^2-y^2}$ occ |
|---------------------------|------------|----------------|-----------|-------------------------------------|-------------------|
| <b>Co-corrole</b>         |            |                |           |                                     |                   |
| $S = 1$                   | 1.84/1.86  | 0.45/0.47      | 0.0       | Co <sup>III</sup> {d <sup>6</sup> } | 0                 |
| $S = 0$                   | 1.84/1.86  | 0.46/0.47      | 6.1       | Co <sup>III</sup> {d <sup>6</sup> } | 0                 |
| $S = 2$                   | 1.84/1.87  | 0.47/0.44      | 25.0      | Co <sup>III</sup> {d <sup>6</sup> } | 0                 |
| <b>Co-corrin</b>          |            |                |           |                                     |                   |
| $S = 0$                   | 1.84/1.89  | 0.52/0.42      | 0.0       | Co <sup>I</sup> {d <sup>8</sup> }   | 0                 |
| $S = 1$                   | 1.85/1.90  | 0.43/0.38      | 10.0      | Co <sup>II</sup> {d <sup>7</sup> }  | 0                 |
| $S = 2$                   | 1.86/1.92  | 0.35/0.30      | 46.0      | Co <sup>II</sup> {d <sup>7</sup> }  | 1                 |
| <b>Co-porphyrin</b>       |            |                |           |                                     |                   |
| $S = 1/2$                 | 1.96       | 0.43           | 0.0       | Co <sup>II</sup> {d <sup>7</sup> }  | 0                 |
| $S = 3/2$                 | 2.00       | 0.35           | 16.9      | Co <sup>II</sup> {d <sup>7</sup> }  | 1                 |
| $S = 5/2$                 | 2.03       | 0.29           | 49.2      | Co <sup>II</sup> {d <sup>7</sup> }  | 1                 |
| <b>Fe-porphyrin</b>       |            |                |           |                                     |                   |
| $S = 1$                   | 1.98       | 0.54           | 0.0       | Fe <sup>II</sup> {d <sup>6</sup> }  | 0                 |
| $S = 0$                   | 1.97       | 0.54           | 12.7      | Fe <sup>II</sup> {d <sup>6</sup> }  | 0                 |
| $S = 2$                   | 2.04       | 0.42           | 14.7      | Fe <sup>II</sup> {d <sup>6</sup> }  | 1                 |

<sup>a</sup> Values for Fe-porphyrin<sup>8</sup> are given for comparison. The occupation of the metal  $d_{x^2-y^2}$  orbital is also given (see text).

**Table 2.** Calculated Minimum Structures for Different Spin States of Co-corrole<sup>a</sup>



| parameter                                      | spin state |         |         | exp <sup>b</sup> |
|--|------------|---------|---------|------------------|
|  | $S = 1$    | $S = 0$ | $S = 2$ |                  |
| Co-N <sub>1</sub>                              | 1.86       | 1.86    | 1.87    | 1.89-1.90        |
| Co-N <sub>2</sub>                              | 1.84       | 1.84    | 1.84    | 1.87             |
| N <sub>1</sub> -C <sub>1</sub>                 | 1.41       | 1.41    | 1.39    | 1.39             |
| N <sub>1</sub> -C <sub>4</sub>                 | 1.39       | 1.38    | 1.39    | 1.40             |
| N <sub>2</sub> -C <sub>6</sub>                 | 1.37       | 1.36    | 1.38    | 1.36             |
| N <sub>2</sub> -C <sub>9</sub>                 | 1.39       | 1.40    | 1.39    | 1.37-1.38        |
| C <sub>9</sub> -C <sub>12</sub>                | 1.40       | 1.39    | 1.43    | 1.41             |
| C <sub>6</sub> -C <sub>7</sub>                 | 1.43       | 1.44    | 1.43    | 1.46             |
| C <sub>7</sub> -C <sub>8</sub>                 | 1.39       | 1.39    | 1.40    | 1.38             |
| C <sub>1</sub> -C <sub>5</sub>                 | 1.39       | 1.39    | 1.41    | 1.42             |
| C <sub>5</sub> -C <sub>6</sub>                 | 1.40       | 1.40    | 1.39    | 1.38-1.40        |
| C <sub>1</sub> -C <sub>2</sub>                 | 1.43       | 1.43    | 1.42    | 1.45             |
| C <sub>2</sub> -C <sub>3</sub>                 | 1.37       | 1.37    | 1.38    | 1.36             |
| C <sub>4</sub> -C <sub>10</sub>                | 1.39       | 1.39    | 1.39    | 1.39             |
| C <sub>5,10</sub> -H                           | 1.09       | 1.09    | 1.09    |                  |
| C <sub>2,3,7,8</sub> -H                        | 1.09       | 1.09    | 1.09    |                  |
| N <sub>2</sub> CoN <sub>4</sub>                | 82.5       | 82.4    | 82.4    | 80.3             |
| N <sub>1</sub> CoN <sub>3</sub>                | 95.1       | 95.4    | 95.5    | 95.2             |
| C <sub>4</sub> C <sub>10</sub> C <sub>11</sub> | 124.1      | 124.1   | 125.0   | 125.8            |
| CoN <sub>1</sub> C <sub>1</sub>                | 126.7      | 126.8   | 127.3   | 126.6-126.9      |
| CoN <sub>2</sub> C <sub>6</sub>                | 133.7      | 134.1   | 133.9   | 131.1-133.5      |
| C <sub>1</sub> C <sub>5</sub> C <sub>6</sub>   | 122.5      | 122.3   | 122.5   | 123.1-123.4      |

<sup>a</sup> Distances and angles are given in angstroms and degrees, respectively. <sup>b</sup> X-ray structure of Co(OMTPC)PPh<sub>3</sub>.<sup>16</sup> The minimum-maximum values for each type of structural parameter are listed.

tions of Co (the Co atom is 0.29 Å out-of-plane toward the PPh<sub>3</sub> axial ligand, which is not present in the computed structure). The similarity between Co(OMTPC)PPh<sub>3</sub> and Co-corrole supports the conclusions of experimental studies that the structure of corrole is not very sensitive to ring substitution.<sup>1</sup> Also worth comparing are the Co-N distances in Co-corrole and the Sc-N lengths obtained in the recent DFT study of Sc-corrole

(18) The corresponding  $\beta$ -unsubstituted complex Co(corrole)PPh<sub>3</sub>, for which structural data are also available,<sup>23</sup> is affected by disorder in the corrin ring.

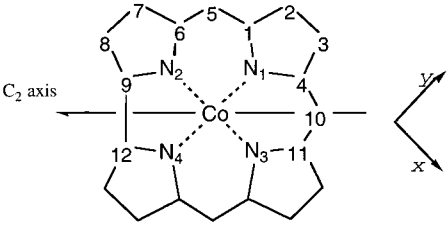
by Ghosh and Jynge<sup>10a</sup> because both molecules are centered around a third-row metal atom. The smaller ionic radius of the Co atom compared to Sc is reflected in the smaller Co–N distances (1.84 Å/1.86 Å in Co-corrole vs 1.96 Å/2.04 Å in Sc-corrole).

The cobalt atom in Co-corrole (Co{d<sup>6</sup>}) is isoelectronic with the iron atom in Fe-porphyrin (Fe{d<sup>6</sup>}), and both systems have an aromatic  $\pi$  system. A priori, one could thus expect some similarities in the electronic structures of Co-corrole and Fe-porphyrin. For Co-corrole in the ground state (the triplet  $S = 1$ ), we found the Co d configuration<sup>19</sup> (d<sub>xy</sub>)<sup>2</sup>(d<sub>z<sup>2</sup></sub>)<sup>2</sup>(d <sub>$\pi_1$</sub> )<sup>1</sup>(d <sub>$\pi_2$</sub> )<sup>1</sup>. The singlet state shows the same configuration, with an antiparallel alignment of the electrons in the last two spin orbitals. This is indeed the same ordering of spin states and the same  $M d$  orbital configuration as were found for Fe-porphyrin,<sup>9a</sup> the only difference being the smaller energy differences between the spin states of Fe-porphyrin. Another peculiarity of Co-corrole compared to Fe-porphyrin is that there is almost no change in the metal–N distances upon a change in spin state (Table 1), whereas a significant lengthening (0.07 Å) was observed in Fe-porphyrin.

Analysis of the spin orbitals of the quintuplet state of Co-corrole reveals that, unlike that of Fe-porphyrin, the metal d<sub>x<sup>2</sup>-y<sup>2</sup></sub> atomic orbital is not occupied. This is not surprising, since this orbital lies quite high in energy in the ground state (0.9 eV from the HOMO), and it also explains the absence of Co–N lengthening for the quintuplet state. In addition, there are two unpaired electrons in spin orbitals of corrole character, which is reflected in the spin density that has a significant contribution from the corrole macrocycle. Overall, the electron configuration of the  $S = 2$  state can be described as (d<sub>xy</sub>)<sup>2</sup>(d<sub>z<sup>2</sup></sub>)<sup>2</sup>(d <sub>$\pi_1$</sub> )<sup>1</sup>(d <sub>$\pi_2$</sub> )<sup>1</sup>-( $\phi^{\text{cor}}$ )<sup>1</sup>( $\phi^{\text{cor}}$ )<sup>1</sup>, where the notations  $\phi^{\text{cor}}$  and  $\phi^{\text{cor}}$  are used to indicate a spin orbital of corrole character. From a comparison with the electron configuration of the ground state, the triplet  $\rightarrow$  quintuplet transition can be regarded as the excitation of one electron from a filled corrole orbital ( $\phi^{\text{cor}}$ ) to an empty one ( $\phi^{\text{cor}}$ ). The first of these orbitals ( $\phi^{\text{cor}}$ ) has strong bonding character with respect to the C<sub>9</sub>–C<sub>12</sub> bond (it includes an in-phase combination of the p<sub>z</sub> orbitals of C<sub>9</sub> and C<sub>12</sub>), while the second one ( $\phi^{\text{cor}}$ ) is C<sub>9</sub>–C<sub>12</sub> antibonding. As a consequence, excitation of one electron from  $\phi^{\text{cor}}$  into  $\phi^{\text{cor}}$  leads to lengthening of the C<sub>9</sub>–C<sub>12</sub> distance in the quintuplet state (Table 2). The above Co d electron configurations (which all correspond to six electrons on the cobalt atom) imply that the formal oxidation state of the cobalt atom is the same for all spin states: Co<sup>III</sup>.

**Co-corrin.** We considered three different spin states of the biologically important Co-corrin (Figure 1b):  $S = 0, 1, 2$ . The lowest energy spin state turned out to be the singlet ( $S = 0$ , closed shell), followed by the triplet ( $S = 1$ ) at 10 kcal/mol and the quintuplet ( $S = 2$ ) at a quite high energy (46 kcal/mol). Table 3 gives selected structural parameters for each spin state. In all cases, the optimization converged to a nonplanar structure of C<sub>2</sub> symmetry. As a measure of the nonplanarity, the “thickness” (the distance between the “highest” and “lowest” carbons, read from their  $z$  coordinates) is 0.80 Å. The corresponding planar structure (optimized with the constraint that all non-hydrogen atoms are in-plane) is considerably higher in energy (74.5 kcal/mol). This is nevertheless an unstable structure, which evolves toward the nonplanar structure once the constraint is released. Three different values for the C–H

**Table 3.** Calculated Minimum Structures for Different Spin States of Co-corrin<sup>a</sup>



| param  | spin state |         |         | exp <sup>b</sup>        |
|--|------------|---------|---------|-------------------------|
|  | $S = 0$    | $S = 1$ | $S = 2$ |                         |
| Co–N <sub>1</sub>                              | 1.89       | 1.90    | 1.92    | 1.91                    |
| Co–N <sub>2</sub>                              | 1.84       | 1.85    | 1.86    | 1.89                    |
| N <sub>1</sub> –C <sub>1</sub>                 | 1.39       | 1.39    | 1.36    | 1.38–1.39               |
| N <sub>1</sub> –C <sub>4</sub>                 | 1.37       | 1.37    | 1.40    | 1.34–1.35               |
| N <sub>2</sub> –C <sub>6</sub>                 | 1.32       | 1.32    | 1.34    | 1.30–1.31               |
| N <sub>2</sub> –C <sub>9</sub>                 | 1.49       | 1.49    | 1.48    | 1.49–1.50               |
| C <sub>9</sub> –C <sub>12</sub>                | 1.52       | 1.52    | 1.53    | 1.56                    |
| C <sub>6</sub> –C <sub>7</sub>                 | 1.51       | 1.51    | 1.51    | 1.51–1.55               |
| C <sub>7</sub> –C <sub>8</sub>                 | 1.54       | 1.54    | 1.54    | 1.55–1.57               |
| C <sub>1</sub> –C <sub>5</sub>                 | 1.37       | 1.37    | 1.40    | 1.39                    |
| C <sub>5</sub> –C <sub>6</sub>                 | 1.41       | 1.41    | 1.39    | 1.44–1.45               |
| C <sub>1</sub> –C <sub>2</sub>                 | 1.51       | 1.51    | 1.51    | 1.53                    |
| C <sub>2</sub> –C <sub>3</sub>                 | 1.53       | 1.53    | 1.53    | 1.55                    |
| C <sub>4</sub> –C <sub>10</sub>                | 1.38       | 1.38    | 1.38    | 1.37–1.39               |
| C <sub>5,10</sub> –H                           | 1.09       | 1.09    | 1.09    | 1.12 (C <sub>10</sub> ) |
| C <sub>2,3,7,8</sub> –H                        | 1.10       | 1.10    | 1.10    |                         |
| C <sub>9,12</sub> –H                           | 1.11       | 1.11    | 1.11    | 1.10 (C <sub>12</sub> ) |
| N <sub>2</sub> CoN <sub>4</sub>                | 83.0       | 82.7    | 83.0    | 83.0                    |
| N <sub>1</sub> CoN <sub>3</sub>                | 94.4       | 94.5    | 95.6    | 96.7                    |
| N <sub>2</sub> CoN <sub>3</sub>                | 172.5      | 172.8   | 171.1   | 172.6                   |
| C <sub>4</sub> C <sub>10</sub> C <sub>11</sub> | 124.5      | 125.0   | 126.6   | 125.6                   |
| CoN <sub>1</sub> C <sub>1</sub>                | 125.5      | 125.2   | 125.7   | 127.0–127.1             |
| CoN <sub>2</sub> C <sub>6</sub>                | 132.5      | 132.0   | 131.3   | 130.4–132.2             |
| C <sub>1</sub> C <sub>5</sub> C <sub>6</sub>   | 122.5      | 122.8   | 122.6   | 120.9–120.8             |

<sup>a</sup>Distances and angles are given in angstroms and degrees, respectively. <sup>b</sup>Neutron structure of vitamin B<sub>12</sub> coenzyme at 15 K.<sup>20</sup> The minimum–maximum values for each type of structural parameter are listed.

lengths are found, the shortest ones (1.09 Å) for the hydrogens attached to C<sub>sp<sup>2</sup></sub> and the longest ones (1.11 Å) for the hydrogens attached to C<sub>9</sub> and C<sub>12</sub>, which suffer from steric hindrance due to the two directly connected pyrroles. As a consequence of this steric interaction, the C<sub>9</sub>–C<sub>12</sub> distance in Co-corrin (0.52 Å) is significantly larger than that in Co-corrole (1.40 Å) and the N<sub>2</sub>CoN<sub>4</sub> angle is slightly more open.

To the best of our knowledge, there is no structural information available for a four-coordinated Co-corrin macrocycle (many B<sub>12</sub> synthetic models are based on noncorrin ligands such as dimethylglyoxime or bis(salicylaldehyde) phenylene diimine<sup>7</sup>). We therefore compared the structure of the free Co-corrin with that of the Co-corrin fragment of the B<sub>12</sub> coenzyme, whose neutron diffraction structure is available.<sup>20</sup> As shown in Table 3, the Co-corrin fragment of B<sub>12</sub> is very similar to the free Co-corrin. The small discrepancies appearing in the Co–N<sub>1</sub> and Co–N<sub>2</sub> distances are probably caused by the two axial ligands of B<sub>12</sub>, which are not present in the free Co-corrin. The similarity between both corrins is easily seen when their three-dimensional structures are compared (see Figure 3). The distortion of the pyrroles is more pronounced in the B<sub>12</sub> Co-corrin than in the free Co-corrin, but the type of conformation is strongly preserved. The largest variation is probably due to the strain induced by the linkage of pyrrole D with the axial

(19) The orbitals labeled as d <sub>$\pi_1$</sub>  and d <sub>$\pi_2$</sub>  refer to the d<sub>xz</sub> + d<sub>yz</sub> and d<sub>xz</sub> – d<sub>yz</sub> combinations, respectively, of the d orbitals of Co (we follow the axis convention given at the top of Table 2). The same notation was used in our previous work on Fe-porphyrin complexes.<sup>9a</sup>

(20) Bouquiere, J. P.; Finney, J. L.; Lehmann, M. S.; Lindley, P. F.; Savage, H. F. J. *Acta Crystallogr., Sect. B* **1993**, *49*, 79–89.

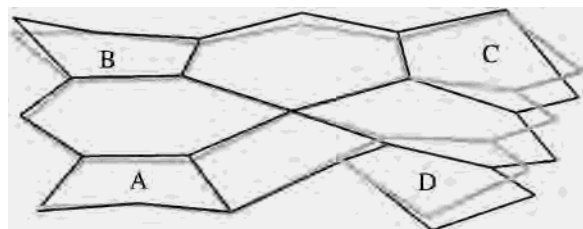


**Figure 3.** Superposition of the optimized structures of the ground states of free Co-corrin (black lines) and the Co-corrin fragment in the B<sub>12</sub> coenzyme (gray lines) extracted from its neutron diffraction structure.<sup>20</sup> The hydrogen atoms have been omitted for clarity. The structures are viewed along a direction slightly tilted with respect to the C<sub>2</sub> axis.

dimethylbenzimidazole ligand in the B<sub>12</sub> coenzyme. Therefore, the structural conformation of the Co-corrin fragment of B<sub>12</sub> appears to be an inherent property of the Co-corrin macrocycle. This contrasts with the porphyrin-based biomolecules, where the main source of heme distortion is attributed to the external forces exerted on the porphyrin ring.<sup>21</sup> It is also worth mentioning that a recent spectroscopic study<sup>5</sup> concluded that corrin conformational changes do not play a decisive role in the function of coenzyme B<sub>12</sub>, in contrast to what has often been assumed.<sup>7</sup> The fact that the Co-corrin conformation in B<sub>12</sub> shows a distortion similar to that of free Co-corrin provides further support for this conjecture.

Small structural changes are observed upon varying the spin state (Table 3). The Co–N distances are 0.02–0.03 Å longer in the quintuplet state ( $S = 2$ ), and there are also variations in the angles, especially on the most flexible side of the ring (opposite to the strained C<sub>9</sub>–C<sub>10</sub> bond). The most noticeable variation occurs in the C<sub>4</sub>C<sub>10</sub>C<sub>11</sub> angle, which is 2.1° larger in the quintuplet state than in the ground state. There is also a small increase in the ring deformation: the N<sub>1</sub>CoN<sub>3</sub> and N<sub>2</sub>–CoN<sub>3</sub> angles change by 1.2–1.4°, and the distance between the “highest” and “lowest” carbons of the macrocycle increases by 0.04 Å. Even more noticeable is the change in the N<sub>1</sub>–C<sub>1</sub>/N<sub>1</sub>–C<sub>4</sub> and C<sub>1</sub>–C<sub>5</sub>/C<sub>5</sub>–C<sub>6</sub> pair of distances, which reverse their length ordering (Table 3). As will be shown below, the reason for these structural changes can be traced back to differences in the electronic structure.

Analysis of the highest occupied spin orbitals of the ground state shows that they have a strong metal character. The cobalt d configuration<sup>19</sup> is  $(d_{xy})^2(d_{\pi 1})^2(d_{\pi 2})^2(d_z)^2$ , as expected for a d<sup>8</sup> metal in a distorted square-planar environment. The  $d_{x^2-y^2}$  orbital is found among the unoccupied orbitals and is quite separate in energy (0.6 eV from the HOMO).

The electron configuration of the triplet state can be best described as  $(d_{xy})^2(d_{\pi 2})^2(d_{\pi 1})^2(d_z)^1(\phi^{\text{corr}})^1$ . This state is characterized by a singly occupied spin orbital of corrin character ( $\phi^{\text{corr}}$ ), which is shown in Figure 4a. This spin orbital was found among the occupied orbitals of the ground state. Thus, from a comparison with the ground-state electron configuration, the overall singlet  $\rightarrow$  triplet transition can be regarded as the excitation of one electron from the  $d_z$  orbital into the empty  $\phi^{\text{corr}}$  orbital. As a consequence, the formal oxidation state of Co changes from Co<sup>I</sup> to Co<sup>II</sup>. This is also reflected in the Mulliken charges: the charge on the corrin ring decreases significantly (–0.7).

In the case of the quintuplet state, a similar analysis leads to the following electron configuration:  $(d_{xy})^2(d_{\pi 2})^2(d_{\pi 1})^2(\phi^{\text{corr}})^1(d_z)^1(\phi^{\text{corr}})^1(d_{x^2-y^2})^1$ , where  $\phi^{\text{corr}}$  is the same orbital as discussed above and  $\phi^{\text{corr}'}$  is a doubly occupied orbital of the ground state

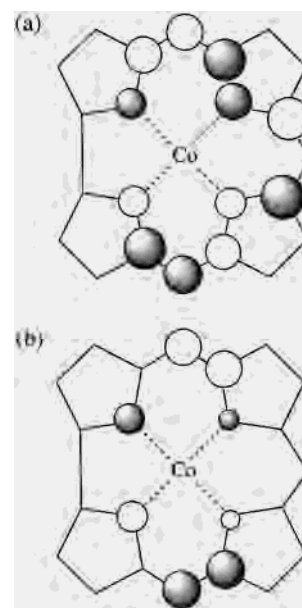


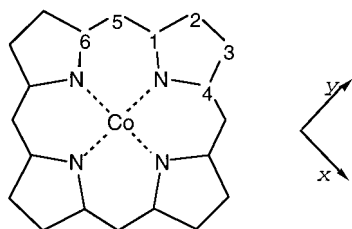
**Figure 4.** (a) Empty orbital of Co-corrin which “receives” one electron in both triplet and quintuplet excited states (referred to as  $\phi^{\text{corr}}$  in the text). The shaded/white pattern is used to distinguish the signs of the atomic p<sub>z</sub> orbitals. (b) Same type of representation for the occupied orbital of the ground state which loses one electron in the quintuplet state (denoted  $\phi^{\text{corr}'}$  in the text).

(the one lying below the Co d orbitals). Because of the presence of two unpaired electrons in the spin orbitals of corrin character (Figure 4), the spin density receives a significant contribution from the corrin macrocycle. Overall, the singlet (ground state)  $\rightarrow$  quintuplet transition can be regarded as the excitation of two electrons from the  $d_z$  and  $\phi^{\text{corr}'}$  orbitals into the  $d_{x^2-y^2}$  and  $\phi^{\text{corr}}$  orbitals. It follows from the above electron configuration (corresponding to eight electrons on the Co atom) that the formal oxidation state of the Co atom (Co<sup>I</sup>) is the same as that of the ground state.

As shown in Figure 4, the  $\phi^{\text{corr}'}$  orbital is antibonding with respect to the N<sub>1</sub>–C<sub>1</sub> bond and strongly bonding with respect to the C<sub>1</sub>–C<sub>5</sub> bond. In contrast,  $\phi^{\text{corr}}$  is N<sub>1</sub>–C<sub>1</sub> bonding and C<sub>1</sub>–C<sub>5</sub> antibonding. Therefore, excitation of one electron from  $\phi^{\text{corr}'}$  to  $\phi^{\text{corr}}$  should shrink the N<sub>1</sub>–C<sub>1</sub> bond and enlarge the C<sub>1</sub>–C<sub>5</sub> bond, which is, indeed, what occurs for the quintuplet state (Table 3). This explains why the ordering N–C<sub>1</sub> > N–C<sub>4</sub> and C<sub>5</sub>–C<sub>6</sub> > C<sub>1</sub>–C<sub>5</sub> reverses in the quintuplet state. On the other hand,  $d_{x^2-y^2}$  occupation is found in the quintuplet state. This orbital has a strong antibonding character with respect to the nitrogen  $\sigma$  lone pairs, and the system thus tries to minimize this repulsion by lengthening the Co–N distances (0.03 Å in Co–N<sub>1,3</sub> and 0.02 Å in Co–N<sub>2,4</sub>) and increasing the ring’s deviation from planarity. The largest Co–N lengthening occurs for the nitrogens far from the rigid C<sub>9</sub>–C<sub>12</sub> bond, which leads to the opening of the C<sub>4</sub>C<sub>10</sub>C<sub>11</sub> angle.

In summary, our calculations show that free Co-corrin is nonplanar (C<sub>2</sub> symmetry), with the same type of conformation as observed in the more complex B<sub>12</sub> coenzyme. Significant electron reorganization, involving excitation to corrin orbitals and change of oxidation state, can be induced by changing the spin state. In particular, the Co atom is in an oxidation state of II in the triplet state, the same oxidation state as in the B<sub>12</sub> coenzyme after the Co–C bond homolysis.

**Co-porphyrin.** The structure of Co-porphyrin (Figure 1c) was optimized by considering the three spin states  $S = 1/2, 3/2, 5/2$ .

**Table 4.** Calculated Minimum Structures for Different Spin States of Co-porphyrin<sup>a</sup>

| param  | spin state |           |           | exp <sup>b</sup> |
|--|------------|-----------|-----------|------------------|
|  | $S = 1/2$  | $S = 3/2$ | $S = 5/2$ |                  |
| Co–N   | 1.96       | 2.00      | 2.03      | 1.97             |
| N–C <sub>1</sub>                             | 1.39       | 1.39      | 1.38      | 1.37             |
| C <sub>1</sub> –C <sub>2</sub>               | 1.44       | 1.44      | 1.43      | 1.44–1.45        |
| C <sub>2</sub> –C <sub>3</sub>               | 1.36       | 1.37      | 1.37      | 1.36             |
| C <sub>1</sub> –C <sub>5</sub>               | 1.38       | 1.39      | 1.40      | 1.37–1.38        |
| C <sub>2,3,5</sub> –H                        | 1.09       | 1.09      | 1.09      |                  |
| CoNC <sub>1</sub>                            | 127.9      | 127.3     | 127.2     | 127.4–128.1      |
| NC <sub>1</sub> C <sub>5</sub>               | 125.1      | 125.2     | 124.4     | 124.7–125.2      |
| NC <sub>1</sub> C <sub>2</sub>               | 111.2      | 110.3     | 110.5     | 110.6–111.8      |
| C <sub>1</sub> C <sub>2</sub> C <sub>3</sub> | 106.7      | 107.0     | 106.7     | 105.9–106.8      |
| C <sub>1</sub> C <sub>5</sub> C <sub>6</sub> | 123.7      | 124.9     | 126.6     | 124.8–125.1      |
| C <sub>1</sub> C <sub>2</sub> H              | 124.3      | 124.7     | 125.0     |                  |
| C <sub>1</sub> C <sub>5</sub> H              | 118.2      | 117.6     | 116.7     |                  |

<sup>a</sup> Distances and Angles Are Given in Angstroms and Degrees, Respectively. <sup>b</sup> X-ray structure of (octaethylporphyrinato)cobalt(II), from ref 22a. The minimum–maximum values for each type of structural parameter are listed.

The low-spin state ( $S = 1/2$ ) was identified as the ground state. This is in agreement with experiments on Co(OEP), Co(TPP), and Co(T<sub>piv</sub>PP),<sup>17,22</sup> in which the only differences with respect to the system considered here are the porphyrin substituents (ethyl, phenyls, and tetrapivalamidophenyl, respectively). The quartet ( $S = 3/2$ ) and sextet ( $S = 5/2$ ) states were found respectively at 16.9 and 49.2 kcal/mol above the ground state (Table 1).

The structure of Co-porphyrin turned out to be planar with  $D_{4h}$  symmetry. The size of the coordination cavity in the ground state (Co–N = 1.96 Å) is significantly larger than those in the corrinoids (1.84/1.89 Å for Co-corrin 1.84/1.86 Å for Co-corrinole), although it is smaller than that Fe-porphyrin (1.98 Å), due to the larger ionic radius of Fe with respect to Co. Thus, a stronger effect on the M–N distances is achieved by changing the macrocycle (corrinoid/porphyrin) than by merely replacing the metal atom (Co/Fe).

As shown in Table 4, the structure is quite insensitive to the spin state, except for the Co–N distances, which are noticeably larger for the excited state. The small increase in the C<sub>1</sub>C<sub>5</sub>C<sub>6</sub> angle is then a consequence of the Co–N lengthening. This is different from what we have found for the cobalt corrinoids (Co-corrin and Co-corrinole), which show very little change in the Co–N distances.

There are several examples of four-coordinate Co-porphyrin derivatives whose X-ray structure is available.<sup>22</sup> We have compared our calculated results with the structure of Co(OEP),<sup>22a</sup> which has an almost planar porphyrin ring (structures with bulky porphyrin substituents, such as Co(TPP) and Co(T<sub>piv</sub>PP),<sup>22b,c</sup> exhibit quite ruffled porphyrin rings). As shown

in Table 4, the structure of the ground-state Co-porphyrin is in excellent agreement with that of Co(OEP).

Analysis of the highest occupied spin orbitals of the ground state displays the Co d orbital configuration  $(d_{xy})^2(d_{xz})^2(d_{yz})^2(d_{z^2})^1$ . The unpaired spin thus lies on the  $d_{z^2}$  atomic orbital of Co. Occupation of the  $d_{x^2-y^2}$  atomic orbital was found in both excited states ( $S = 3/2$ ,  $S = 5/2$ ), which explains the lengthening of the Co–N distances (Table 4). Another feature of Co-porphyrin is that the  $d_{z^2}$  orbital (half-filled in the ground state) becomes doubly occupied in both quartet and sextet states. The electron orbital configuration can be described as  $(d_{xy})^2(d_{z^2})^2(d_{xz})^1(d_{yz})^1(d_{x^2-y^2})^1$  for the  $S = 3/2$  state and  $(d_{xy})^2(d_{z^2})^2(d_{xz})^1(d_{yz})^1(d_{x^2-y^2})^1(\phi^{\text{porph}})^1(\phi^{\text{porph}'})^1$  for the  $S = 5/2$  state, where the labels  $\phi^{\text{porph}}$  and  $\phi^{\text{porph}'}$  refer to orbitals centered on the porphyrin ring. Thus, the ground state  $\rightarrow$  quartet excitation can be regarded as the transfer of two electrons from  $d_{xz}$  and  $d_{yz}$  (both filled) into  $d_{z^2}$  (half-filled) and  $d_{x^2-y^2}$  (empty), respectively. Further excitation from a filled porphyrin  $\pi$  orbital ( $\phi^{\text{porph}}$ ) to an empty one ( $\phi^{\text{porph}'}$ ) occurs in the sextet state. None of these porphyrin orbitals exhibit sizable bonding or antibonding character among neighboring porphyrin atoms, and thus *no significant changes in the C–C or C–N distances are observed in Co-porphyrin upon changing the spin state, in contrast to what was found in the corrinoids*. Similarly as in Co-corrinole and Fe-porphyrin but in contrast to the case of Co-corrin, the oxidation state of the metal atom (Co<sup>II</sup>) of Co-porphyrin does not change with spin state.

## Final Remarks

We have analyzed the structural and electronic properties of Co-porphyrin, Co-corrinole, and Co-corrin. Structure optimizations were performed, with no symmetry constraints, accounting for different spin states of each macrocycle:  $S = 0, 1, 2$  for Co-corrinole and Co-corrin and  $S = 1/2, 3/2, 5/2$  for Co-porphyrin. The lowest energy spin states were found to be of intermediate spin for Co-corrinole ( $S = 1$ ) but of low spin for Co-corrin ( $S = 0$ ) and Co-porphyrin ( $S = 1/2$ ).

The  $\pi$  aromatic systems, Co-corrinole and Co-porphyrin, turn out to be planar with respectively  $C_{2v}$  symmetry and  $D_{4h}$  symmetry (which was also found in Fe-porphyrin<sup>9a</sup>). In contrast, the Co-corrin deviates considerably from planarity and displays  $C_2$  symmetry (Figure 4a).

An excellent agreement of the computed structure with experiment is found for Co-porphyrin, for which an X-ray structure with the same type of cobalt coordination is available. This gives us some confidence in the precision of the computed structures of the four-coordinate Co-corrin and Co-corrinole, for which structural data are not yet available. Nevertheless, the computed structure of free Co-corrinole is also in good agreement with that of the five-coordinate Co(OMTPC)PPh<sub>3</sub>,<sup>16</sup> This weak dependence on coordination could be a consequence of the weak tendency of corrolates to distort because of steric effects (which are due to either the presence of bulky corrinole substituents or the crystal packing) as has been discussed in ref 1.

The nonplanar conformation of free Co-corrin is quite similar to that of the Co-corrin fragment of the B<sub>12</sub> coenzyme.<sup>20</sup> This brings us to the conclusion that the structure of the Co-corrin macrocycle is responsible for most of the distortion of the Co-corrin core of the B<sub>12</sub> coenzyme. On the other hand, this is also an indication of the low sensitivity of Co-corrin to steric interactions, which is at variance with the proposed occurrence of such interactions between the corrin ring and the 5'-deoxyadenosyl ligand in the B<sub>12</sub> coenzyme.<sup>7</sup> Nevertheless, our results support the conclusions of a recent spectroscopic study<sup>5</sup> that excluded the key role of such steric interactions.

- (22) (a) Scheidt, W. R.; Turowska-Tyrk, I. *Inorg. Chem.* **1994**, *33*, 1314–1318. (b) Madura, P.; Scheidt, W. R. *Inorg. Chem.* **1994**, *33*, 3182. (c) Collman, J. P.; Gagne, R. R.; Kouba, J.; Ljusberg-Wahren, H. J. *Am. Chem. Soc.* **1974**, *96*, 6800.  
(23) Hitchcock, P.; McLaughlin, G. *J. Chem. Soc., Dalton Trans.* **1976**, 1927.

The computed M–N distances (Co- and Fe-porphyrin (1.96–1.98 Å) > Co-corrin, Co-corrinole (1.84–1.89 Å)) are in agreement with the empirical observation that shorter M–N distances are found in corrinoids than in porphyrins. Comparing Fe with Co for the same macrocycle (Co- and Fe-porphyrin), we observe a larger M–N distance (0.02 Å) for Fe, consistent with its larger ionic radius compared to that of Co. However, the M–N increase achieved by replacing Co with Fe is smaller than that obtained by replacing the corrinoid with a porphyrin macrocycle (0.7–0.10 Å).

Compared to the porphyrins analyzed here (Co- and Fe-porphyrin), the corrinoids (Co-corrinole and Co-corrin) exhibit a lower sensitivity to changes in the Co–N distances (see Table 1). Occupation of the  $d_{x^2-y^2}$  orbital leads, in all cases, to the lengthening of the Co–N distances (i.e., for the  $S = 2$  state of Co-corrin and for the  $S = 3/2, 5/2$  states of Co-porphyrin), but this effect is much less pronounced in the corrinoids than in the porphyrins. (As shown in Table 1,  $d_{x^2-y^2}$  occupation increases the Co–N distances by 0.03 Å in Co-corrin, 0.04–0.07 Å in Co-porphyrin, and 0.06 Å in Fe-porphyrin.) The difference in sensitivity of the M–N distances of Co-corrin and Co-porphyrin to  $d_{x^2-y^2}$  occupation is probably due to the difference in rigidity of the rings. In the case of Co-corrin, the orbital repulsion associated with  $d_{x^2-y^2}$  occupation is less pronounced than that in Co-porphyrin, since the corrin ring is not planar (the overlap between the  $d_{x^2-y^2}$  orbital and the nitrogen  $\sigma$  orbitals is smaller than that for a planar ring). Moreover, the antibonding character of the  $d_{x^2-y^2}$  orbital can be diminished not only by enlarging the Co–N distances but also by increasing the deviation of the ring from planarity). In the case of Co-porphyrin (and also Fe-porphyrin), the aromaticity of the ring forces it to be planar and  $d_{x^2-y^2}$  occupation has a major effect on enlarging the metal–nitrogen distances.

It is also notable that there is a large excitation energy associated with  $d_{x^2-y^2}$  occupation in the corrinoids (46 kcal/mol for the quintuplet Co-corrin, according to Table 1) compared to the porphyrins (14.7–16.9 kcal/mol). The reasons for this behavior could be the stronger ligand field of the corrinoids and the rigidity of the central  $\text{CoN}_4$  core (due to the two directly connected pyrroles), both of which cause the  $d_{x^2-y^2}$  orbital to

lie very high in energy. As a consequence, this orbital rarely becomes occupied when the spin state is increased (in the only case where the  $d_{x^2-y^2}$  is occupied, the energy rises considerably). In contrast, the changes in the spin states of the corrinoids are accompanied by electron excitation from Co d orbitals into empty ring orbitals (as in the triplet Co-corrin) or from filled ring orbitals into empty ring orbitals (as in quintuplet-state Co-corrinole and Co-corrin). These electronic excitations can lead to small changes in the carbon-ring structure, without strongly affecting the M–N distances. This can shed some light on the question of why nature chooses Co-corrin in the  $\text{B}_{12}$  coenzyme and not porphyrin as in many other biomolecules (e.g., myoglobin, hemoglobin, or the cytochromes).

In relation to this question, it is worth recalling the relevance of such M–N variations to the function of myoglobin or hemoglobin. The release of oxygen causes a change in the spin state of the Fe-porphyrin from a singlet to a quintuplet, in which the  $d_{x^2-y^2}$  orbital is occupied. Simultaneously, the iron atom moves out-of-plane and the Fe–N distances increase. It seems rather obvious, given the properties discussed above, that a corrinoid macrocycle would not be suitable for this function.

In conclusion, our results demonstrate the absence of significant steric constraints on the corrin ring of the  $\text{B}_{12}$  coenzyme and underline the different responses of corrinoids and porphyrins to changes in the size of the coordination cavity. This study represents the first quantitative assessment of structural and electronic properties of Co-corrinole, Co-corrin, and Co-porphyrin, and it is a first step toward the modeling of the more complex  $\text{B}_{12}$  coenzyme and of the electronic/structural rearrangements accompanying the Co–C bond homolysis.

**Acknowledgment.** This work was supported by the Max-Planck-Institut and the CNRS. Computer resources were provided by the Scientific Committee of the Institut du Développement et des Ressources en Informatique Scientifique, Orsay, France. We thank P. Ballone for suggesting this study and for his help in its initial stage. We are also indebted to E. Canadell for useful discussions and careful reading of the original manuscript.

IC000143M